Desalination and Water Treatment
www.deswater.com

doi: 10.5004/dwt.2017.20912

80 (2017) 276–287
June

An insight into the prediction of biosorption mechanism, and isotherm, kinetic and thermodynamic studies for Ni(II) ions removal from aqueous solution using acid treated biosorbent: the *Lantana camara* fruit

K. Nithya[a,*], Asha Sathish[b], P. Senthil Kumar[c], T. Ramachandran[b]

[a]*Department of Chemical Engineering and Materials Science, Amrita School of Engineering, Amrita Vishwa Vidyapeetham, Amritanagar P. O., Coimbatore 641112, India, Tel. +91 9443477623; email: nithiamrita@gmail.com*
[b]*Department of Sciences, Amrita School of Engineering, Amrita Vishwa Vidyapeetham, Amritanagar P.O., Coimbatore 641112, India, Tel. +91 9943977361/+91 9942006690; emails: s_asha@cb.amrita.edu (A. Sathish), t_ramachandran@cb.amrita.edu (T. Ramachandran)*
[c]*Department of Chemical Engineering, SSN College of Engineering, Chennai 603 110, India, Tel. +91 9884823425; email: senthilchem8582@gmail.com*

Received 3 December 2016; Accepted 9 May 2017

ABSTRACT

The study focuses on exploring the binding mechanisms of Ni(II) ions and determining the maximum uptake capacity of the biosorbent. The fresh biosorbent was subjected to sulfuric acid treatment to enhance the porosity and to introduce the specific sulfonic groups onto the surfaces of the biosorbent. Characterization techniques like scanning electron microscope, energy-dispersive X-ray spectroscopy, Fourier transform infrared spectroscopy and elemental analysis were utilized to understand the biosorption mechanisms. The results exhibit the likelihood of both physical and chemical interactions of the biosorbent with the Ni(II) ions. Out of the isotherm models investigated, Langmuir model presented a better fit to the experimental data favoring monolayer adsorption. In addition, intra-particle diffusion model revealed the possibility of both pore and film diffusion. Compared with pseudo–first-order model, pseudo-second-order kinetic model obtained a better fit. The outcome of the thermodynamic studies showed the exothermic nature of the biosorption process with a negative enthalpy value ($\Delta H°$). Additionally, it is also significant to note that the adsorption of Ni(II) ions was favored only at lower temperatures. A maximum removal efficiency of 97% was observed for 25 mg/L Ni(II) solution. Moreover, the results of the desorption studies using 0.3 N HCl were also encouraging, with a removal efficiency of almost 91%.

Keywords: Biosorption; Nickel; Mechanism; Isotherm; *Lantana*; Thermodynamics

1. Introduction

Heavy metals presences are considered as one of the global concerns among the various pollutants due to their toxicity and persistence in the environment [1,2]. These metals, released into the environment through various anthropogenic sources, contaminate water bodies and ultimately cause irreparable damage to human health and environment. In recent years, much focus has been put on understanding the toxicity of heavy metals and lot of effort is exercised toward addressing the problem of wastewater generation caused because of the indiscriminate release of the effluents containing heavy metals.

Electroplating sector involving too many heavy metals (chromium, nickel, cadmium, zinc, copper, etc.,) and their derivatives, is one of the leading causes of heavy metal pollution. In addition, the use of nickel is also extended in industries such as paint formulation, non-ferrous metal, porcelain enameling, copper sulfate manufacture, steam-electric power plants and mineral processing [3,4]. Specifically, nickel,

* Corresponding author.

on exceeding the discharge limits, leads to health hazards such as renal edema, lung cancer, pulmonary fibrosis, skin dermatitis and gastrointestinal discomfort [5,6]. However, a permissible amount of nickel is indeed involved in significant metabolic reactions of living organisms. According to Bureau of Indian Standard (BIS), the permissible discharge level of industrial effluent containing Ni(II) ions into the land water is 3.0 mg/L [7,8]. Further, it should also be noted that according to the World Health Organization guidelines, Ni(II) ions in drinking water should not exceed a value of 0.5 mg/L [9].

The conventional methods designed for the removal of Ni(II) ions include adsorption, ion exchange, membrane technologies, evaporation, electrochemical treatment, chemical reduction and precipitation. However, these treatments are quite expensive and some technologies even result in unwanted by-products. Presently biosorption, an alternative technology, is spreading widely among researchers due to its low cost and appreciable results even at lower metal ion concentrations. Biosorption is the process of utilizing dead biomass for the removal of heavy metals from aqueous solutions. However, in general, the biosorption mechanism is complex, involving complexation, ion exchange, precipitation, physical adsorption and chelation. Some of the biosorbents investigated on Ni(II) ions include raw and modified coir pith [10], black carrot residues [11], cashew nut shell [12], *Parthenium hysterophorus L.* activated carbon [13], rice husk [14], *Sphagnum peat* biomass [15], etc.

In this research, the chemically modified biosorbent was prepared from the fruit of an exotic weed namely *Lantana camara,* considered to be a lurking menace in Mudumalai Tiger Reserve [16]. This *L. camara* plant species seen throughout central and southern part of India has tiny black colored fruits of 5 mm diameter and is mainly found in dry stony hills and black soil [16,17]. The selected biosorbent was also pretreated with acid to improve the efficiency and to obtain enhanced adsorption capacity. This pretreated biosorbent earlier investigated for the removal of Cr(VI) from aqueous solution exhibited improved adsorption capacity [16]. In the present investigation, to carry out equilibrium, kinetic and thermodynamic studies, batch scale experiments were conducted on selected parameters. This resulted in optimum contact time, pH, biosorbent dosage, temperature and metal ion concentration. In addition, regeneration studies were also carried out using 0.3 N HCl as a desorbing agent to ensure the economic feasibility and applicability of the selected biosorbent.

2. Materials and methods

2.1. Preparation of biosorbent

The sample preparation procedure carried out was detailed in our previous paper [16]. The fresh *L. camara* fruits were water washed, dried and crushed to obtain a uniform particle size of 150 μm. The resulted product is considered to be the fresh biosorbent and later, it is treated with concentrated sulfuric acid. This pretreated material is referred to as chemically treated *L. camara* (CTLC) biosorbent. The fresh biosorbent and CTLC biosorbent used in the present study were referred to as LC1 and LC2 biosorbent, respectively, in our previous paper [16]. Pretreatments are widely known for enhancing the adsorptive capacity of heavy metals and hence used in our study. Moreover, chemical activation using sulfuric acid at moderate temperatures is also claimed for producing enhanced surface area and better adsorption characteristics [18,19].

2.2. Biosorbent characterization

The investigation of the biosorption mechanism and the surface morphology of the fresh and CTLC biosorbent before and after biosorption were explored using scanning electron microscope (SEM-Carl Zeiss, Sigma version). Additionally, energy-dispersive X-ray spectroscopy (EDX) analysis was also performed to understand the elemental composition. The results of the EDX analysis were also supported by elemental analysis (Elementar, Vario Micro Cube). The surface area, maximum pore volume and pore width of the biosorbents were determined using, Micromeritics, ASAP 2010, surface area and porosity analyzer. The distribution of Ni(II) ions on the biosorbent surface was also figured out using EDX studies. Furthermore, Fourier transform infrared spectroscopy (FTIR; Nicolet IS 10, USA) was utilized to study the possible functional groups in the fresh biosorbent and to understand the transformations after chemical modification and biosorption of Ni(II) ions. The wavelength used for the study ranged from 4,000 to 400 cm^{-1}.

2.3. Batch-mode experiments

Stock solution of Ni(II) is prepared to a concentration of 1,000 mg/L by dissolving 4.48 g of $NiSO_4 \cdot 6H_2O$ in 1,000 mL of pure distilled water. This stock solution is used to prepare solutions of various concentrations such as 25, 50, 100, 150 and 200 mg/L. pH was adjusted using digital pH meter (Systronic). Exempting thermodynamic studies, all the batch level experiments were conducted at a constant temperature of 303 K. The adsorbate volume was continued to be 50 mL for an agitation speed of 160 rpm. Required amount of sample and Ni(II) solution of known concentration were taken in 250 mL Erlenmeyer flask and allowed for shaking in the orbital incubator shaker (SLM-INC-OS-250). Later, after the attainment of equilibrium the flasks were removed from the shaker and the adsorbate was filtered using Whatman filter paper (no. 41).

To conduct various isotherm studies, the Ni(II) ion concentrations (25, 50, 100, 150 and 200 mg/L) with an optimal dose of 0.8 g and pH of 5 were investigated. It should also be noted that the equilibrium period was maintained to be 70 min. Moreover, kinetic and thermodynamic studies (303, 313, 323 and 333 K) were carried out under the same optimal conditions for 25 mg/L concentration of Ni(II) solution. The Ni(II) ion concentration before and after the biosorption process was determined using atomic absorption spectrophotometer. The calculation of biosorbent adsorptive capacity was determined using the equation:

$$q_e = \frac{(C_0 - C_e)V}{m} \quad (1)$$

In the above equation, C_0 is the initial Ni(II) ions concentration, C_e is the equilibrium Ni(II) ions concentration, m is the

biosorbent dosage (g), V denotes the volume of Ni(II) solution (L) and q_e refers to the equilibrium adsorptive capacity (mg/g).

2.4. Biosorbent regeneration/desorption studies

The effective deployment of biosorption for the removal of heavy metals from industrial wastewater is possible only on successful regeneration of the biosorbent. The results of the significant factors influencing the economic feasibility of the biosorption process is desorption of metal ions from aqueous solution. The desorption potential of CTLC biosorbent was investigated using 0.3 N HCl at a temperature of 303 K. Compared with various acid-based desorbing agents, HCl is proven to be an effective desorbent in the removal of Ni(II) ions. This is also shown by the results reported earlier [20]. The eluent and the metal loaded biosorbent were allowed to be contacted for 70 min at 160 rpm speed. Eventually, the Ni(II) ion loaded CTLC biosorbent was separated from the eluent after desorption and washed with distilled water.

3. Results and discussions

3.1. Biosorbent characterization

The biosorption of Ni(II) ions for fresh and CTLC biosorbent were revealed by the EDX spectrum image as given in Figs. 1(a)–(d). The occurrence of Ni(II) ions was observed in both the nickel loaded fresh and CTLC biosorbent. 1 of the EDX analysis were in accordance with the elemental analysis data as shown in Table 1 revealing the presence of carbon, hydrogen, oxygen, nitrogen and sulfur. The SEM image of the fresh biosorbent without any chemical activation was characterized by rough flat irregular surfaces embedded with minute pores (Fig. 2(a)). But soon after biosorption, the flat surfaces disappeared and created several haphazard aggregated structures, attributing to the binding of Ni(II) ions (Fig. 2(b)). Whereas, in the chemically activated biosorbent, the likelihood of intra-particle diffusion mechanism was established by the presence of internal pores which were then occupied by Ni(II) ions (Fig. 2(c)). However, these pores were seen to be broken and randomly distributed in the biosorbent. This variably sized pores lead to wide spread surface area and trap metal ions efficiently. The enlarged cavities resulted after the biosorption processes validate the possibility of the internal diffusion of Ni(II) ions into the CTLC biosorbent (Fig. 2(d)). These pores are further evidenced in the results of Brunauer, Emmett and Teller (BET) analysis shown in Table 2. The studied adsorbents being macroporous (pore size > 50 nm) have a low surface area. Nevertheless for porous adsorbents, pore volume and pore size plays an active role in adsorption than the surface area. Hence, pore volume and pore width are on the higher end compared with the surface area as shown in Table 2.

The occurrence of major functional groups such as carbohydrates, glycosides and flavonoids were established

Table 1
Carbon, hydrogen, nitrogen and sulfur (CHNS) elemental analysis for fresh and CTLC biosorbent

Sample	Fresh biosorbent	Acid treated biosorbent
Carbon (%)	45.67	56.12
Hydrogen (%)	6.178	4.807
Oxygen (%)	46.60	36.76
Nitrogen (%)	1.53	–
Sulfur (%)	–	2.31

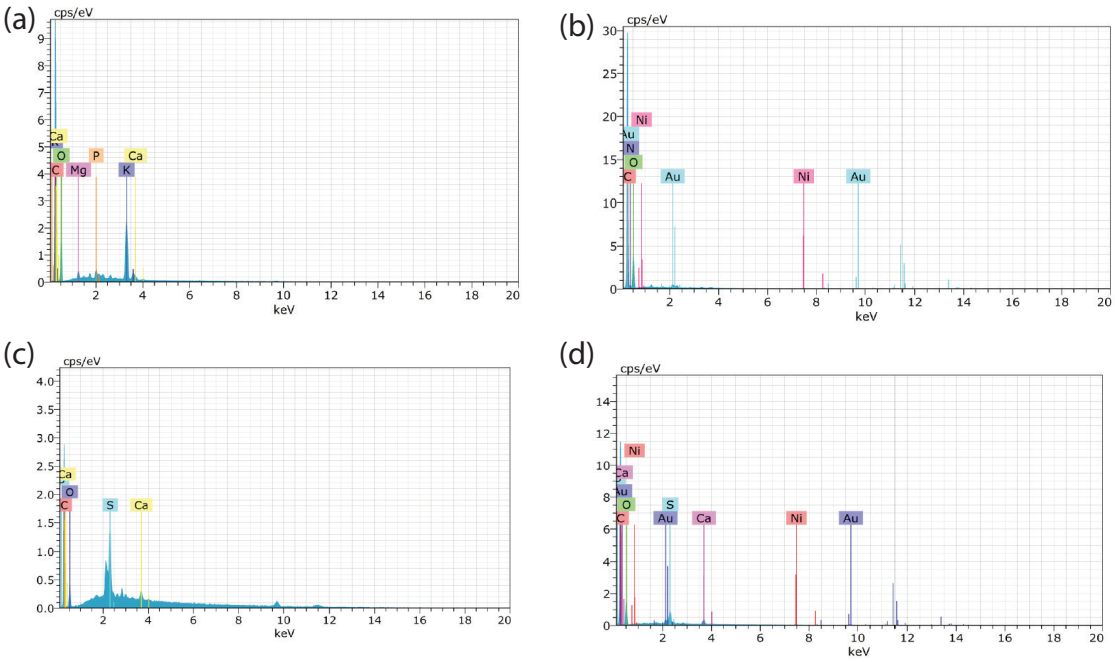

Fig. 1. EDX pictures of (a) fresh biosorbent, (b) adsorbate loaded fresh biosorbent, (c) CTLC biosorbent and (d) adsorbate loaded CTLC biosorbent.

with the help of IR spectra as shown in Fig. 3. The FTIR band positions of the fresh biosorbent and their corresponding shift of peaks after biosorption are tabulated in Table 3. In the fresh biosorbent, a peak of 1,037 cm^{-1} corresponds to C–OH stretching vibration and the band for 3,395 cm^{-1} relates to the identification of OH and N–H stretch. Further, free hydroxyl group is assured by the presence of a sharp peak at 3,700 cm^{-1}. Also, a band around 1,424 cm^{-1} attributes to the aromatic C=C group confirming the occurrence of flavonoids and glycosides in the fresh biosorbent. Further, the presence of C=O group in amide is evidenced by the peak seen around 1,646 cm^{-1}. Based on the results obtained from the FTIR spectra of adsorbate loaded fresh biosorbent as shown in Fig. 4, the hydrogen bonded hydroxyl band and NH band (3,395–3,417 cm^{-1}) exhibited significant shift in the band position; whereas the free hydroxyl group in the IR spectra showed only mild changes after the adsorption of Ni(II) ions in the fresh biosorbent. On the other hand, the results of the FTIR study of CTLC biosorbent (Table 4) indicate that no major functional groups were lost after sulfuric acid treatment as shown in Fig. 5. It is a well-known fact that sulfuric acid is a strong dehydrating agent and the biosorbent on acid treatment will have strong influence on hydroxyl group and amide group. This is shown by the major shift in band frequency (3,395–3,437 cm^{-1}). Furthermore, the emergence of new peaks around 1,160 and 1,030 cm^{-1} attributes to the sulfonate groups resulted from the sulfuric acid treatment. Also, the vibrational frequency of CTLC biosorbent before and after biosorption is compared and remarkable changes were observed in the adsorbate loaded CTLC biosorbent as shown in Fig. 6. The involvement of hydroxyl groups (3,437–3,419 cm^{-1}) and carbonyl groups (1,641–1,629 cm^{-1}) in the removal of metal ions is clearly shown by the shifting of band frequencies to lower wave numbers as shown in Table 4. In addition, the contribution of the free OH group in the removal of metal ions is also revealed by the disappearance of the peak around 3,741 cm^{-1}. Major shifts were also found in the CH stretching vibration (1,458–1,391 cm^{-1}) suggesting the influence of all the dominant functional groups. Additionally, the peak for aromatic C=C group (1,545–1,535 cm^{-1}) exhibited significant shift contributing to the biosorption of Ni(II) ions.

Table 2
Brunauer, Emmett and Teller (BET) analysis for fresh and CTLC biosorbent

Type of biosorbent	Surface area (m^2/g)	Pore width (Å)	Maximum pore volume (cm^3/g)
Fresh biosorbent	0.0850	1,874.258	0.001063
Acid treated biosorbent	0.1829	4,769.257	0.011452

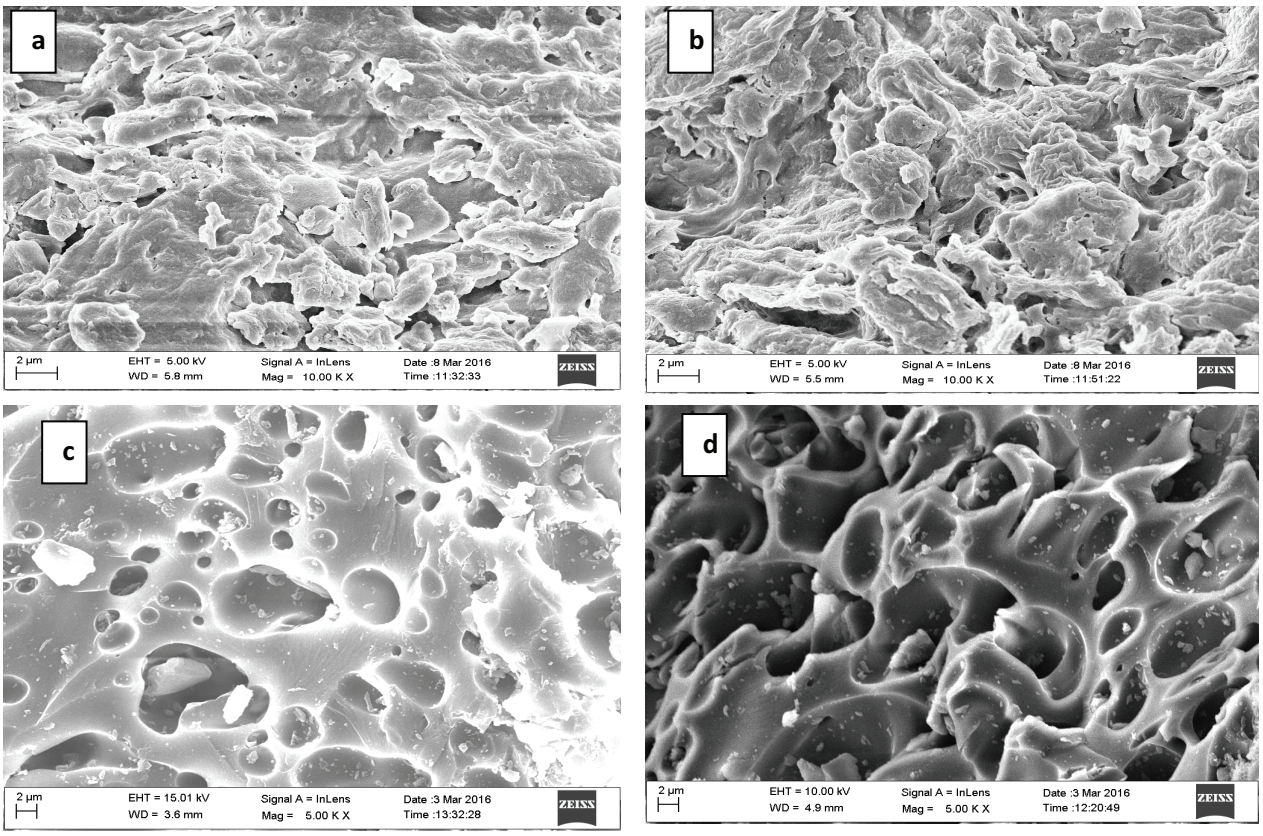

Fig. 2. SEM pictures of (a) fresh biosorbent, (b) adsorbate loaded fresh biosorbent, (c) CTLC biosorbent and (d) adsorbate loaded CTLC biosorbent.

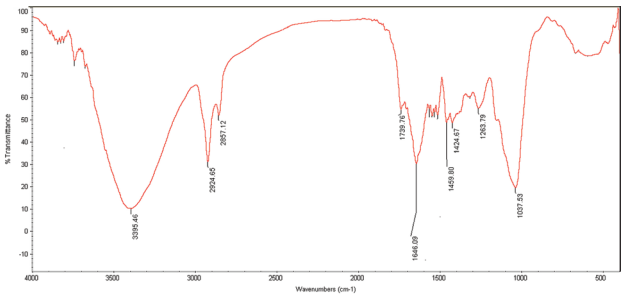

Fig. 3. FTIR spectra of fresh biosorbent.

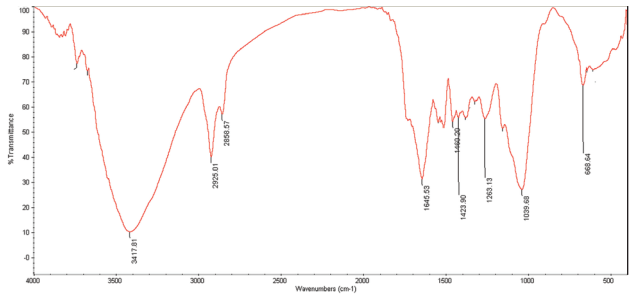

Fig. 4. FTIR spectra of Ni(II) ions loaded fresh biosorbent.

Table 3
FTIR band position for fresh biosorbent on biosorption

Band position (cm)	Shifted band position (cm)	Major functional groups
3,395.46	3,417.81	OH group and N–H stretch
2,925.01	Not shifted	=C–H stretch
2,857.12	2,858.57	=C–H stretch
1,646.09	1,645.53	C=O stretch/N–H bending
1,459.80	1,460.20	C–H vibration
1,424.67	1,423.90	C=C in aromatic compounds
1,263.79	1,263.13	Stretching vibration of C–OH
1,037.53	1,039.68	Stretching vibration of C–OH

Table 4
FTIR band position for CTLC biosorbent on biosorption

Band position (cm)	Shifted band position (cm)	Major functional groups
3,437.39	3,419.31	OH group and N–H stretch
2,924.21	2,924.09	=C–H stretch
2,855.48	2,855.45	=C–H stretch
1,641.24	1,629.02	C=O stretch/N–H bending
1,545.59	1,535.0	C=C in aromatic compounds
1,458.67	1,391.53	C–H vibration
1,160.78	1,100.00	S=O stretch
1,030.81	1,027.64	Stretching vibration of C–OH/S=O stretch

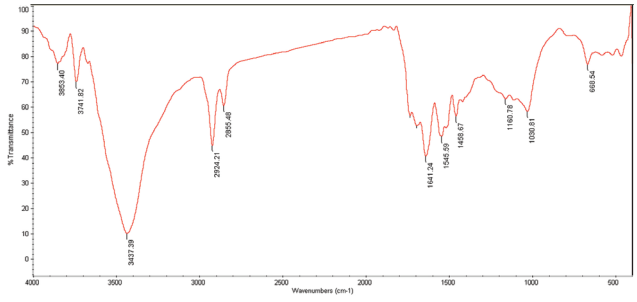

Fig. 5. FTIR spectra of CTLC biosorbent.

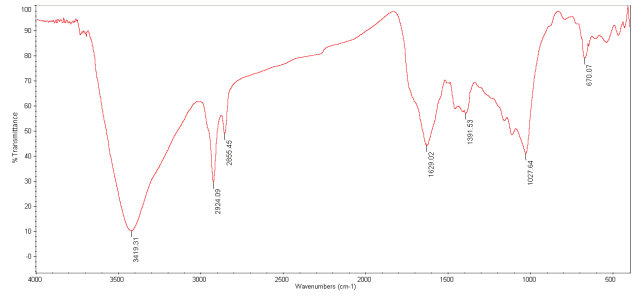

Fig. 6. FTIR spectra of Ni(II) ions loaded CTLC biosorbent.

3.2. Batch mode experiments

The Ni(II) removal efficiency from the aqueous solution was examined for concentrations starting from 25 to 200 mg/L. The optimum pH, biosorbent dosage and contact time at which the experiments were carried out is based on the results of the batch experiments (figure not shown). The fresh biosorbent yielded a removal efficiency of 72% for 25 mg/L nickel solution at an optimal dose of 0.8 g and a pH of 5 with 70 min contact time. On the other hand, a maximum removal of 97% is observed for the acid treated biosorbent under the same conditions. Hence, further investigations on isotherm, thermodynamic and kinetic studies were conducted for CTLC biosorbent.

3.3. Isotherm studies

3.3.1. Langmuir adsorption model

This isotherm earlier used for activated carbon adsorption especially for gas–solid systems, now finds its application extensively in the field of biosorption [21]. According to this isotherm model, it is assumed that biosorption could occur only at definite active sites which are identical. In other words, it emphasizes on monolayer adsorption without involving any kind of interaction even between their lateral surfaces [22]. The equation for Langmuir isotherm model is as follows [21]:

$$\frac{1}{q_e} = \frac{1}{q_{\max} b C_e} + \frac{1}{q_{\max}} \quad (2)$$

The above equation defines q_{max} (mg/g) as the maximum adsorption capacity and C_e (mg/L) as the equilibrium concentration of Ni(II) ions.

A dimensionless constant (R_L) called as separation factor is defined by the following equation [23]:

$$R_L = \frac{1}{1 + b\,C_0} \tag{3}$$

This constant helps in determining the viability of biosorption where b (L/mg) refers to the Langmuir constant and C_0 denotes the initial Ni(II) ion concentration. According to the values exhibited in Table 5 the removal of Ni(II) ions on using CTLC biosorbent showcases a favorable trend. This is based on the fact that when R_L value falls between 0 and 1 the isotherm is said to be favorable. If separation factor (R_L) value greater than 1 is obtained, then the biosorption is said to be unfavorable and when equal to zero, the isotherm becomes irreversible. Linear isotherm is further possible when R_L value equals to 1 [24].

The slope and intercept of the plot ($1/q_e$ vs. $1/C_e$) in Fig. 7 obtain the value for maximum adsorption capacity and the Langmuir constant. A better fit with a higher coefficient of determination value of 0.99 was exhibited for the Langmuir plot as shown in Fig. 7. It shows the possibility of monolayer adsorption of adsorbate molecules onto the surfaces of the biosorbent. Often, monolayer adsorption is associated with chemisorption and hence the likelihood of chemical adsorption is predominant on the removal of Ni(II) ions. A lower Langmuir constant generally shows greater credibility in the removal of metal ions through adsorption. In this context, a lower value of 0.109 L/mg (Table 6) confirms the selectivity of CTLC in removing Ni(II) ions from aqueous solution. The calculated metal uptake capacity also conforms to the experimented values as shown in Table 6, representing the better applicability of this model in the studied biosorption process.

Table 5
Calculated Langmuir separation factor (R_L) for the biosorption of Ni(II) using CTLC biosorbent

Initial concentration of Ni(II) (mg/L)	Separation factor (R_L) derived from Langmuir isotherm
25	0.0045
50	0.0028
100	0.0011
150	0.0007
200	0.0004

3.3.2. Freundlich adsorption model

Contrary to the above model, this model supposes multilayer adsorption, where biosorption occurs over heterogeneous surfaces [25]. According to this isotherm, the biosorbent will not attain any saturation phase with adsorbate ions, whereas the surface coverage is infinite [26].

The linearized form of the Freundlich equation for adsorption of liquids is described by the following equation:

$$\log q_e = (1/n)\log C_e + \log K_F \tag{4}$$

In this model, C_e implies Ni(II) ion equilibrium concentration (mg/L), q_e refers to equilibrium adsorption capacity (mg/g), K_F represents Freundlich constant relating to adsorption capacity and $1/n$ refers to Freundlich constant corresponding to adsorption intensity [27]. These constants K_F and $1/n$ were calculated from the intercept and the slope correspondingly from the plot of $\log q_e$ vs. $\log C_e$ (Fig. 8).

Based on the plot $\log q_e$ vs. $\log C_e$, the obtained coefficient of determination value of 0.91 suggests the likelihood of heterogeneous adsorption. However, the experimental uptake capacity did not exactly match with the calculated metal uptake capacity values as shown in Table 6. The mechanism of adsorption could be chemical adsorption if a value of n^{-1} less than 1 is obtained. This is supported from Table 6 which shows a value of 0.319 suggesting chemisorption. Altogether, based on the results obtained, this model can also be suggested as a reasonable model for the study of Ni(II) ions using the selected biosorbent. The applicability of this model also shows that the mechanism of adsorption in the present study is not restricted to monolayer adsorption.

3.3.3. Dubinin–Radushkevich model

This empirical model is usually appreciable to understand the mechanism of adsorption approaching Gaussian energy distribution over heterogeneous surfaces [28,29]. Contrary to the other two models investigated, this model is completely temperature dependent, which is one of its distinctive features [24]. Moreover, this isotherm is exclusively used to distinguish the physical and chemical adsorption. The model is expressed as shown below in the equation:

$$q_e = q_{m,D}\exp(-K_{DR}\,\varepsilon^2) \tag{5}$$

The value for ε is calculated using the following equation:

$$\varepsilon = RT\ln\left[1 + \frac{1}{C_e}\right] \tag{6}$$

Table 6
Significant parameters of various isotherm studies for the biosorption of Ni(II) onto CTLC biosorbent

	Langmuir model	Freundlich model	Dubinin–Radushkevich model
Calculated parameters	q_{max} = 5.29 mg/g b = 0.109 L/mg	K = 1.10 (mg$^{1-(1/n)}$ L$^{1/n}$/g) n = 3.130 and n^{-1} = 0.319	$q_{m,D}$ = 4.69 mg/g E = 316 kJ/mol
Coefficient of determination	R^2 = 0.99	R^2 = 0.91	R^2 = 0.96

The mean biosorption energy of biosorption (E) can be arrived using the equation:

$$E = 1/\sqrt{2K_{DR}} \quad (7)$$

Maximum adsorption capacity is represented as $q_{m,D}$ (mg/g), Polanyi potential is denoted as ε (J/mol), C_e refers to Ni(II) ion equilibrium concentration (mg/L), R and T are related to gas constant (8.314 J/mol/K) and absolute temperature (K), respectively. In addition, E, the mean biosorption energy of biosorption (J/mol) is calculated using $K_{DR,}$ Dubinin–Radushkevich constant (mol²/J²). It is established that the mean biosorption energy value between 8 and 16 kJ/mol is justified for ion exchange process, a value lesser than 8 kJ/mol corresponds to physical adsorption and a value greater than 16 kJ/mol indicates particle diffusion [30,31].

The plot between $\ln q_e$ and ε^2 is as shown in Fig. 9. A R^2 value of 0.96 represents a reasonable fit to the experimental data. Moreover, the experimental maximum uptake capacity value exhibits a good match with the theoretical value of this model as shown in Table 6. A mean biosorption energy of 316 kJ/mol (>16 kJ/mol) suggests the likelihood of particle diffusion.

3.4. Biosorption kinetics

The kinetics of the biosorption process was studied using pseudo-first-order, pseudo-second-order kinetic models and intra-particle diffusion model. Biosorption mechanism is completely based on the physical and chemical properties of biosorbent and mass transfer from the bulk fluid phase [32,33]. Pseudo–first-order and pseudo-second-order models help in the understanding of this biosorption mechanism. In addition, it also compares the experimental adsorption capacity with the adsorption capacity obtained from the kinetic model. Furthermore, intra-particle diffusion model is also investigated to explore the boundary layer and the intra-particle diffusion effect.

3.4.1. The pseudo-first-order and pseudo-second-order kinetic models

The linear form of pseudo-first-order kinetic model is given in the equation [34]:

$$\log\left(q_e - q_t\right) = \log q_e - \frac{k_1 t}{2.303} \quad (8)$$

The rate constants k_1 (min^{-1}) and equilibrium adsorption capacity q_e (mg/g) are calculated from the slope and intercept of the plot $\log(q_e - q_t)$ vs. t (Fig. 10). In the above equation, q_t represents the amount of Ni(II) ions adsorbed after time t, expressed in mg/g. This model assumes that the rate of occupied adsorbed sites is proportional to the number of unoccupied sites [35].

Pseudo-second-order model assumes that the rate controlling mechanism is surface-based chemical adsorption involving chemical and physical interactions between the adsorbent and adsorbate [36,37].

The kinetic equation for pseudo-second-order kinetic model is as follows [27]:

$$\frac{dq_t}{dt} = k\left(q_e - q_t\right)^2 \quad (9)$$

Integrating Eq. (9) and on applying boundary conditions, gives Eq. (10):

$$\left(\frac{1}{q_e - q_t}\right) = \frac{1}{q_e} + kt \quad (10)$$

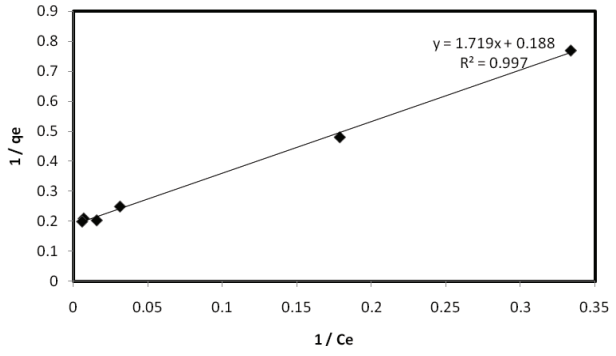

Fig. 7. Langmuir plot for the adsorption of Ni(II) ions.

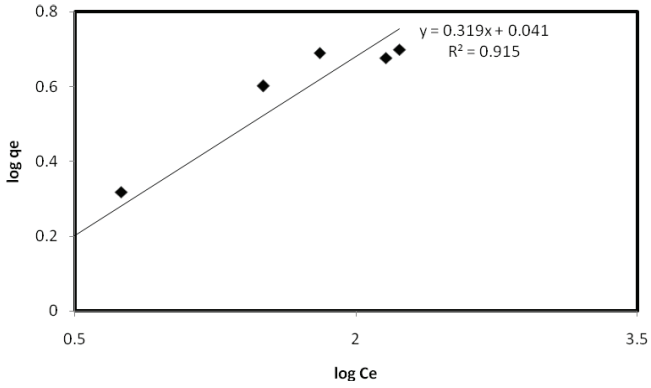

Fig. 8. Freundlich plot for the adsorption of Ni(II) ions.

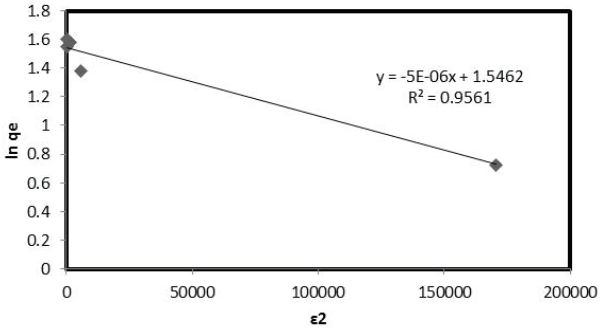

Fig. 9. Dubinin–Radushkevich model for the adsorption of Ni(II) ions.

Eq. (10) may be rearranged to obtain a linear form Eq. (11):

$$\frac{t}{q_t}=\frac{1}{h}+\frac{1}{q_e}t \tag{11}$$

It should be noted that q_e, k and h were determined from the slope and the intercept of the plot t/q_t vs. t, respectively (Fig. 11). The rate constant is defined as k (g/mg/min) and h equal to kq_e^2 (mg/g/min) is considered as the initial adsorption rate as time (t) tends to zero.

In many cases, the adsorption studies usually develop a rapid initial phase due to availability of more active sites which is later followed by a slower phase due to saturation of adsorption sites [38]. Likewise, in the present study, the percentage removal of metal ions in the initial phase was rapid for the first 30 min. It later leads to a slower phase which shows up to 70 min, followed by a saturation phase (figure not shown). However, some systems in particular may consume invariably much longer time to reach equilibrium [39].

These models were investigated to identify the biosorption kinetics and the mechanism. Out of the two models studied, pseudo-second-order model produces a best fit with a higher R^2 value of 0.99. In addition, the experimental adsorption capacity and the uptake capacity calculated from the pseudo-second-order model seem to be almost equal (Table 7). Nevertheless, the calculated adsorption capacity of pseudo-first-order model is not far-off from the experimental values. As the rate of reaction follows pseudo-second-order model, the possibility for chemical adsorption to occur is more prevalent. This involves sharing or exchanging of electrons between CTLC and Ni(II) ions. Furthermore, this represents the contribution of both CTLC dosage and initial Ni(II) ion concentration in influencing the removal of these selected metal ions from aqueous solution.

3.4.2. Intra-particle diffusion model

The equation for intra-particle diffusion model is explained by Weber and Morris [40]. This model supposes that if the rate-limiting step is intra-particle diffusion, a plot of $t^{0.5}$ vs. q_t should obtain a straight line that passes through the origin [41]:

$$q_t = k_{\text{ipd}}\, t^{1/2} + C_i \tag{12}$$

Intra-particle diffusion rate constant (mg/g min$^{1/2}$) is expressed as k_{ipd}, and C_i is the intercept at stage i referring to boundary resistance. It emphasizes that both film diffusion and diffusion within the biosorbent govern the intra-particle diffusion mechanism [42].

The applicability of intra-particle diffusion model is studied to understand the internal and external diffusion mechanism of Ni(II) ions onto the CTLC biosorbent. This model obtained the highest R^2 value next to the pseudo-second-order model (Table 7). Based on the plot shown in Fig. 12 different zones were observed attributing to different mechanisms. Initially a curved pattern is observed followed by a linear pattern, which ultimately lead to a plateau. The curved pattern could be due to boundary layer diffusion effect (physisorption, ion exchange, etc.) and linear pattern is because of the intra-particle diffusion processes (diffusion through micropores and macropores of the biosorbent). The diffusion of

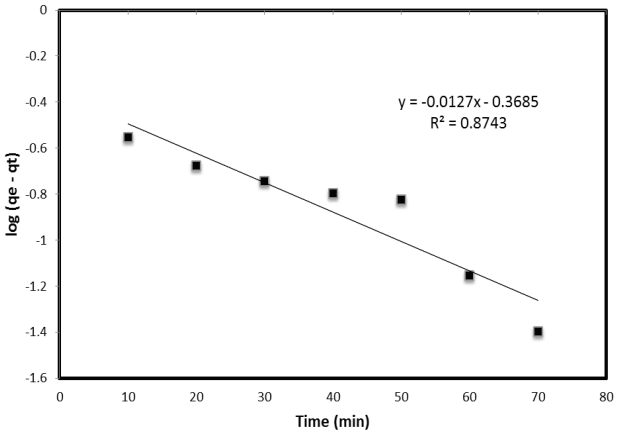

Fig. 10. Pseudo-first-order model for the adsorption of Ni(II) ions.

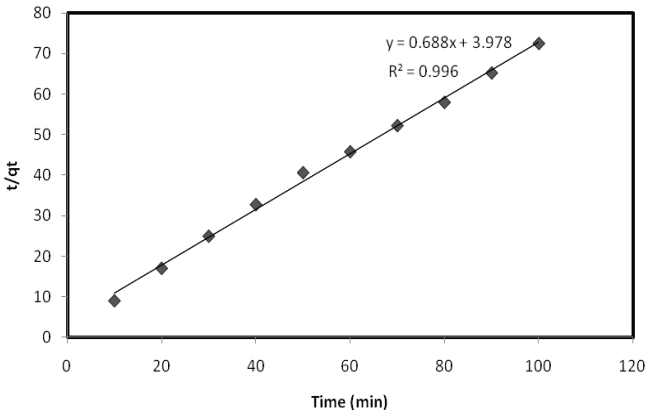

Fig. 11. Pseudo-second-order model for the adsorption of Ni(II) ions.

Table 7
Significant values calculated through various kinetic models

Significant values at a temperature of 303 K for initial Ni(II) concentration of 25 mg/L									
Pseudo-first-order model			Pseudo-second-order model			Intra-particle diffusion model			Experimental
R^2	k_1 (min)	q_e (cal) (mg/g)	R^2	k_2 (g/mg/min)	q_e (cal.) (mg/g)	R^2	k_{ipd} (mg/g/min$^{1/2}$)	C_i (mg/g)	q_e (exp.) (mg/g)
0.87	0.029	2.34	0.99	0.1190	1.45	0.96	0.0439	0.96	1.30

metal ions onto the pores is also evident from the SEM micrograph as shown in Fig. 2(d). Further, the results of Dubinin–Radushkevich model discussed above also strengthen the possibility of particle diffusion. However, it is evident from Fig. 12 that the intra-particle diffusion mechanism is not the sole process in the removal of Ni(II) ions, as the curve is not completely linear and does not pass through origin.

3.5. Thermodynamic studies

Based on the experimental investigations, thermodynamic parameters such as changes in enthalpy ($\Delta H°$), entropy ($\Delta S°$), and change in Gibbs free energy ($\Delta G°$) were calculated. All these factors help to determine the spontaneity of the process and explore whether the adsorption system releases or absorbs heat [43]. These significant thermodynamic parameters were calculated based on the plot ($\ln K_C$ vs. $1/T$) as in Fig. 13, and using the following equation:

$$\Delta G^0 = -RT\ln K_C \tag{13}$$

$$\ln K_C = \frac{-\Delta H^0}{RT} + \frac{\Delta S^o}{R} \tag{14}$$

$$K_C = \frac{C_{Ae}}{C_e} \tag{15}$$

In the above equations, K_C represents the distribution coefficient, R relates to the gas constant (8.314 J/mol/K), T refers to the absolute temperature (K), C_{Ae} is the concentration of Ni(II) ions on the adsorbent at equilibrium (mg/L) and C_e is the concentration of Ni(II) ions in the liquid solution at equilibrium (mg/L). The activation energy (E_a) is the minimal energy required for the interaction of adsorbate with the adsorbent. This is also considered as one of the significant factors in thermodynamic studies [44]. Moreover, the magnitude of E_a helps in determining the type of adsorption. The activation energy will be determined according to the Arrhenius equation as follows:

$$\ln K_C = \ln A - E_a/RT \tag{16}$$

A is called the frequency factor and E_a refers to the activation energy (kJ/mol). It is found that the increase in temperature shows a decreasing trend in the adsorption of Ni(II) ions revealing the exothermic nature of biosorption. This phenomenon is also supported by a negative enthalpy value ($\Delta H°$). Similar trend is seen in the adsorption study of Ni(II) ions using acid treated algal biomass [45]. This could be because of the weakening of adsorptive force between adsorbent and adsorbate and may also be due to the destruction of active adsorption sites at elevated temperatures [46–48]. It should also be noted that as adsorption proceeds effectively at lower temperatures, a very low value of activation energy is obtained. Moreover, the magnitude of activation energy (Table 8) suggests the possibility of film diffusion mechanism in the biosorption process studied [49]. Furthermore,

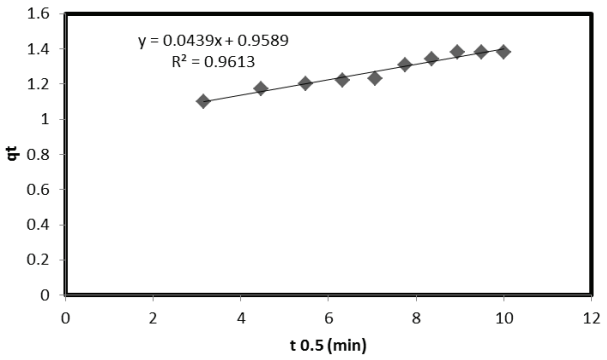

Fig. 12. Intra-particle diffusion model for the adsorption of Ni(II) ions.

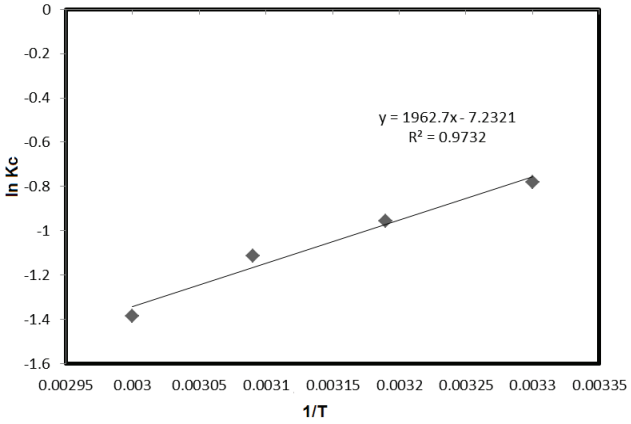

Fig. 13. Thermodynamic plot for the biosorption of Ni(II) ions.

a negative $\Delta S°$ value shown in Table 8 indicates the decreased disorderliness in the solid–liquid interface which may cause adsorbate ions to escape from solid phase back to the liquid phase at higher temperatures [44]. Furthermore, a positive value of $\Delta G°$, implies that the biosorption process is non-spontaneous in the studied temperature range (Table 8). Related trend is also seen in the removal of cadmium ions using sawdust [50]. Considering all the above facts, it could be concluded that the biosorption of CTLC biosorbent on Ni(II) ions is not possible at higher temperatures but lower temperatures favor better adsorption.

3.6. Biosorption mechanism

The presence of alkali and alkaline earth metals, such as potassium, sodium, calcium and magnesium, was confirmed based on the results of the EDX analysis of the fresh biosorbent. However, the images of these peaks completely disappeared in the metal loaded fresh biosorbent. This is an indication for ion exchange of the light metals with the cationic Ni(II) ions. But the EDX images of the CTLC biosorbent varied significantly compared with the fresh biosorbent and hence the mechanism varied invariably. Though acid treatment resulted in enlarged pores, it also damaged most of the inorganic matter and hence no peaks pertaining to light minerals were seen in the EDX image of the CTLC biosorbent except for calcium. These findings were also in accordance

with the earlier study [59]. In view of that, the possibility of ion exchange with the light metals is ruled out in the biosorption mechanism of CTLC biosorbent. However, numerous ligands due to hydroxyl group generate negative sites in the biosorbent at a higher pH of 5 attracting the positively charged Ni(II) ions onto the biosorbent surface, resulting in improved adsorption. This was evidenced by the shift in the hydroxyl group of the FTIR spectra. This electrostatic attraction suggests the possibility of physical adsorption in the CTLC biosorbent. The results of intra-particle diffusion model which claims for the diffusion of metal ions into the pores of the adsorbent also suggests the likelihood of physical adsorption. This is further supported by the mean biosorption energy obtained from the Dubinin model favoring particle diffusion. These pores of the biosorbent were firmly established by SEM images and BET analysis. It shows that the size of these pores was large enough to allow the diffusion of Ni(II) ions into the pores.

Additionally, the presence of H^+ ions in the sulfonic acid group on the surface of the biosorbent was revealed from the results of the FTIR. Hence, it is confirmed that sulfuric acid treatment increases the cation exchange capacity of the biosorbent, leading to the ion exchange of Ni^{2+} with the acidic groups present on the surfaces. Similar tendency is further explained in the biosorption of Ni(II) ions using wheat straw [60]. Later, on saturation of these sites, the metal ions may diffuse into the pores of the biosorbent as mentioned earlier. On the other hand, the hydroxyl group of the biosorbent containing lone pair of electrons in the oxygen atom may also coordinate with positively charged Ni(II) ions leading to the formation of nickel complexes (O–Ni) on the surfaces of CTLC biosorbent. The presence of hydroxyl group in the biosorbent was already confirmed by the results of FTIR study. These findings put forth the possibility of chemical adsorption. This is supported by the results of pseudo-second-order model and Langmuir isotherm studies with a very high R^2 value of 0.99. On the whole, it could be concluded that the biosorption of CTLC biosorbent is extremely complex, involving both physical and chemical adsorption. However, satisfied results were obtained in desorption studies on using acid-based desorbing agent explaining the predominance of physical adsorption.

In addition, the maximum monolayer adsorption capacities of some of the other studied biosorbents are shown in Table 9. Some biosorbents reported highest adsorption capacities than the currently used adsorbent. However, the desorption results of the present study using 0.3 N HCl were highly efficient than most of the other biosorbents. Moreover, our study also differs in the aspect that, more investigations were carried out on the basis of exploring the biosorption mechanism behind the removal of Ni(II) ions.

3.7. Biosorbent regeneration/desorption studies

Biosorption–desorption experimentations were conducted on metal loaded CTLC using HCl as an eluent. The desorption efficiency elevated on increasing HCl concentration from 0.1 to 0.3 N and a maximum removal efficiency of 91% was observed. This increase in HCl concentration accelerates the buildup of H^+ ions and promotes concentration gradient of Ni(II) and H^+ ions favoring ion exchange for desorption process [61]. The results of desorption are encouraging and it emphasizes the need to extend the batch scale setup to industrial studies for real-time applications.

Table 8
Thermodynamic parameters calculated for 25 mg/L Ni(II) ion concentration

Temperature (K)	$\Delta G°$ (kJ/mol)	$\Delta S°$ (kJ/mol/K)	$\Delta H°$ (kJ/mol)	E_a (kJ/mol)
303	1.96	–0.060	–16.31	–1.96
313	2.49			
323	2.99			
333	3.83			

Table 9
Maximum adsorption capacities of the selected biosorbents for the adsorption of Ni(II) ions

Biosorbent	q_{max} (mg/g)	References
Maple sawdust	0.294	[51]
Phosphate treated sawdust	0.70	[52]
Sugarcane bagasse	2.23	[53]
Expanded perlite	2.24	[54]
Oak tree sawdust	3.37	[55]
Acid treated *Lantana camara* fruit	5.29	Our study
Rice husk	5.52	[14]
Groundnut shells	7.49	[56]
Cassava peel	57.07	[57]
Modified corn silk	76.92	[58]

4. Conclusions

The plant *L. camara*, widespread in and around India, is a harmful weed, possessing serious threat to the ecosystem. Hence, the biomass derived from such kind of plant material was chosen for the present study. The biomass was treated with sulfuric acid to improve the cation-exchange and adsorption capacity. Batch level experiments were done to investigate on the kinetic and equilibrium parameters. In addition to that, the mechanisms involved in the biosorption of metal ions were also investigated by exploring several characterization techniques like SEM, EDX and FTIR. Elemental analysis was also performed to reaffirm some of the results of the FTIR study and to understand the elemental composition. The major functional groups of the biosorbent were found to be glycosides, flavonoids and carbohydrates. The results of the FTIR study showed the involvement of almost all of these groups in the biosorption process. Batch scale studies show the equilibrium contact time to be 70 min at an optimum pH of 5 and a maximum removal efficiency of 97%. The influence of temperature has a great deal to do with the adsorption of Ni(II) ions exhibiting decreased efficiency at higher temperatures. Furthermore, the non-spontaneous and exothermic nature of the biosorption process is revealed by the results of the thermodynamic studies. The adsorption of Ni(II) ions fitted better to Langmuir model compared with the Freundlich adsorption model. Furthermore, the results of Dubinin–Radushkevich model also

obtained higher value of coefficient of determination. The most appropriate kinetic model is found to be pseudo-second-order model in comparison with the pseudo-first-order model based on the higher R^2 value. In addition to the physical adsorption the results also favor chemical adsorption in the removal of Ni(II) ions. Also, the results of intra-particle diffusion model confirm the possibility of both film and internal diffusion of Ni(II) ions. In addition, desorption on using HCl was also highly encouraging. Hence, further studies will be conducted on scaling up of batch studies to continuous column study for industrial wastewater applications.

References

[1] V. Janaki, S. Kamala-Kannan, K. Shanthi, Significance of Indian peat moss for the removal of Ni(II) ions from aqueous solution, Environ. Earth Sci., 74 (2015) 5351–5357.

[2] B. Prabhu Dass Batvari, S. Kamala-Kannan, K. Shanthi, R. Krishnamoorthy, K.J. Lee, M. Jayaprakash, Heavy metals in two fish species (*Carangoidel malabaricus* and *Belone stronglurus*) from Pulicat Lake, North of Chennai, Southeast Coast of India, Environ. Monit. Assess., 145 (2008) 167–175.

[3] V. Padmavathy, P. Vasudevan, S.C. Dhingra, Biosorption of nickel(II) ions on Baker's yeast, Proc. Biochem., 38 (2003) 1389–1395.

[4] US Environmental Protection Agency, Treatability Manual, Vol. 1, EPA, Washington, D.C., USA 1988, pp. 4.11–4.12.

[5] M. Torab-Mostaedi, M. Asadollahzadeh, A. Hemmati, A. Khosravi, Equilibrium, kinetic, and thermodynamic studies for biosorption of cadmium and nickel on grapefruit peel, J. Taiwan Inst. Chem. Eng., 44 (2013) 295–302.

[6] A. Çelekli, H. Bozkurt, Bio-sorption of cadmium and nickel ions using *Spirulina platensis*: kinetic and equilibrium studies, Desalination, 275 (2011) 141–147.

[7] S. Congeevaram, S. Dhanarani, J. Park, M. Dexilin, K. Thamaraiselvi, Biosorption of chromium and nickel by heavy metal resistant fungal and bacterial isolates, J. Hazard. Mater., 146 (2007) 270–277.

[8] C.E. Rodríguez, A. Quesada, Nickel biosorption by *Acinetobacter baumannii* and *Pseudomonas aeruginosa* isolated from industrial wastewater, Braz. J. Microbiol., 37 (2006) 465–467.

[9] World Health Organization (WHO), Guidelines for drinking-water quality, Incorporating First Addendum to 3rd Edition, Recommendations, Vol. 1, World Health Organization, Geneva, 2006, p. 595.

[10] A. Ewecharoen, P. Thiravetyan, W. Nakbanpote, Comparison of nickel adsorption from electroplating rinse water by coir pith and modified coir pith, Chem. Eng. J., 137 (2008) 181–188.

[11] F. Güzel, H. Yakut, G. Topal, Determination of kinetic and equilibrium parameters of the batch adsorption of Mn(II), Co(II), Ni(II) and Cu(II) from aqueous solution by black carrot (*Daucus carota* L.) residues, J. Hazard. Mater., 153 (2008) 1275–1287.

[12] P.S. Kumar, S. Ramalingam, S.D. Kirupha, A. Murugesan, T. Vidhyadevi, S. Sivanesan, Adsorption behavior of nickel(II) onto cashew nut shell: equilibrium, thermodynamics, kinetics, mechanism and process design, Chem. Eng. J., 167 (2011) 122–131.

[13] H. Lata, V.K. Garg, R.K. Gupta, Sequestration of nickel from aqueous solution onto activated carbon prepared from *Parthenium hysterophorus* L., J. Hazard. Mater., 157 (2008) 503–509.

[14] K.K. Krishnani, X. Meng, C. Christodoulatos, V.M. Boddu, Biosorption mechanism of nine different heavy metals onto biomatrix from rice husk, J. Hazard. Mater., 153 (2008) 1222–1234.

[15] Y. Kalmykova, A.M. Strömvall, B.M. Steenari, Adsorption of Cd, Cu, Ni, Pb and Zn on *Sphagnum peat* from solutions with low metal concentrations, J. Hazard. Mater., 152 (2008) 885–891.

[16] K. Nithya, S. Asha, P.S. Kumar, T. Ramachandran, Biosorption of hexavalent chromium from aqueous solution using raw and acid-treated biosorbent prepared from *Lantana camara* fruit, Desal. Wat. Treat., 57 (2016) 25097–25113.

[17] T. Venkatachalam, V. Kishorkumar, P. Kalaiselvi, A.O. Maske, N. Senthilkumar, Physicochemical and preliminary phytochemical studies on the *Lantana camara* (L.) fruits, Int. J. Pharm. Sci., 3 (2011) 52–54.

[18] A. Fernando, S. Monteiro, F. Pinto, B. Mendes, Production of biosorbents from waste olive cake and its adsorption characteristics for Zn^{2+} ion, Sustainability, 1 (2009) 277–297.

[19] M. Kobya, E. Demirbas, E. Senturk, M. Ince, Adsorption of heavy metal ions from aqueous solutions by activated carbon prepared from apricot stone, Bioresour. Technol., 96 (2005) 1518–1521.

[20] R.M. Kulkarni, V. Shetty, G. Srinikethan, Cadmium(II) and nickel(II) biosorption by *Bacillus laterosporus* (MTCC 1628), J. Taiwan Inst. Chem. Eng., 45 (2014) 1628–1635.

[21] I. Langmuir, The constitution and fundamental properties of solids and liquids, J. Am. Chem. Soc., 38 (1916) 2221–2295.

[22] K. Vijayaraghavan, T.V.N. Padmesh, K. Palanivelu, M. Velan, Biosorption of nickel(II) ions onto *Sargassum wightii*: application of two-parameter and three-parameter isotherm models, J. Hazard. Mater., 133 (2006) 304–308.

[23] K.R. Hall, L.C. Eagleton, A. Acrivos, T. Vermeulen, Pore-and solid-diffusion kinetics in fixed-bed adsorption under constant-pattern conditions, Ind. Eng. Chem. Res., 5 (1966) 212–223.

[24] K.Y. Foo, B.H. Hameed, Insights into the modeling of adsorption isotherm systems, Chem. Eng. J., 156 (2010) 2–10.

[25] A.W. Adamson, A.P. Gast, Physical Chemistry of Surfaces, 6th ed., Wiley-Interscience, New York, 1997.

[26] Z. Rawajfih, N. Najwa, Characteristics of phenol and chlorinated phenols sorption onto surfactant-modified bentonite, J. Colloid Interface Sci., 298 (2006) 39–49.

[27] P.S. Kumar, S. Ramalingam, V. Sathyaselvabala, S.D. Kirupha, S. Sivanesan, Removal of copper(II) ions from aqueous solution by adsorption using cashew nut shell, Desalination, 266 (2011) 63–71.

[28] A. Gunay, A. Ertan, T. Ismail, Lead removal from aqueous solution by natural and pretreated clinoptilolite: adsorption equilibrium and kinetics, J. Hazard. Mater., 146 (2007) 362–371.

[29] A. Dąbrowski, Adsorption — from theory to practice, Adv. Colloid Interface Sci., 93 (2001) 135–224.

[30] K. Saltalı, A. Sarı, M. Aydın, Removal of ammonium ion from aqueous solution by natural Turkish (Yıldızeli) zeolite for environmental quality, J. Hazard. Mater., 41 (2007) 258–263.

[31] R. Ahmed, T. Yamin, M.S. Ansari, S.M. Hasany, Sorption behaviour of lead(II) ions from aqueous solution onto Haro river sand, Adsorpt. Sci. Technol., 24 (2006) 475–486.

[32] Metcalf and Eddy, Wastewater Engineering Treatment and Reuse, 4th ed., Tata McGraw-Hill, New Delhi, India, 2003.

[33] P. Sujatha, V. Kalarani, B. Naresh Kumar, Effective biosorption of nickel(II) from aqueous solutions using *Trichoderma viride*, J. Chem., 2013 (2013) 1–7.

[34] S. Lagergren, About the theory of so-called adsorption of soluble substances, K. Sven. Vetensk.akad Handl., 24 (1898) 1–39.

[35] C.C. Cruz, A.C.A. da Costa, C.A. Henriques, S. Luna, Kinetic modeling and equilibrium studies during cadmium biosorption by dead *Sargassum sp.* biomass, Bioresour. Technol., 91 (2004) 249–257.

[36] D. Robati, Pseudo-second-order kinetic equations for modeling adsorption systems for removal of lead ions using multi-walled carbon nanotube, J. Nanostruct. Chem., 3 (2013) 1–6.

[37] H. Wang, A. Zhou, F. Peng, H. Yu, J. Yang, Mechanism study on adsorption of acidified multiwalled carbon nanotubes to Pb(II), J. Colloid Interface Sci., 316 (2007) 277–283.

[38] M. Torab-Mostaedi, M. Asadollahzadeh, A. Hemmati, A. Khosravi, Equilibrium, kinetic, and thermodynamic studies for biosorption of cadmium and nickel on grapefruit peel, J. Taiwan Inst. Chem. Eng., 44 (2013) 295–302.

[39] Y.S. Ho, Review of second-order models for adsorption systems, J. Hazard. Mater., 136 (2006) 681–689.

[40] W.J. Weber, J.C. Morris, Kinetics of adsorption on carbon from solution, J. Sanit. Eng. Div., 89 (1963) 31–60.

[41] V.J.P. Poots, G. McKay, J.J. Healy, The removal of acid dye from effluent using natural adsorbents—I peat, Water Res., 10 (1976) 1061–1066.

[42] Y. Onal, C. Akmil-Başar, C. Sarıcı-Ozdemir, Investigation kinetics mechanisms of adsorption malachite green onto activated carbon, J. Hazard. Mater., 146 (2007) 194–203.
[43] M. Tuzen, A. Sarı, Biosorption of selenium from aqueous solution by green algae (*Cladophora hutchinsiae*) biomass: equilibrium, thermodynamic and kinetic studies, Chem. Eng. J., 158 (2010) 200–206.
[44] P. Saha, S. Chowdhury, Insight into Adsorption Thermodynamics, INTECH Open Access Publisher, China, 2011, pp. 349–364.
[45] V.K. Gupta, A. Rastogi, A. Nayak, Biosorption of nickel onto treated alga (*Oedogonium hatei*): application of isotherm and kinetic models, J. Colloid Interface Sci., 342 (2010) 533–539.
[46] A.K. Shroff, V.K. Vaidya, Kinetics and equilibrium studies on biosorption of nickel from aqueous solution by dead fungal biomass of *Mucor hiemalis*, Chem. Eng. J., 171 (2011) 1234–1245.
[47] R. Rajalakshmi, S. Subhashini, P. Lalitha, Usefulness of activated carbon prepared from industrial wastes in the removal of nickel from aqueous solution, J. Chem., 6 (2009) 361–370.
[48] A. Ozer, D. Ozer, Comparative study of the biosorption of Pb(II), Ni(II) and Cr(VI) ions onto *S. cerevisiae*: determination of biosorption heats, J. Hazard. Mater., 100 (2003) 219–229.
[49] T. Sismanoglu, S. Pura, Adsorption of aqueous nitrophenols on clinoptilolite, Colloids Surf., A, 180 (2001) 1–6.
[50] A.B. Albadarin, C. Mangwandi, G.M. Walker, S.J. Allen, M.N. Ahmad, Biosorption characteristics of sawdust for the removal of Cd(II) ions: mechanism and thermodynamic studies, Chem. Eng. Trans., 24 (2011) 1297–1302.
[51] S.S. Shukla, L.J. Yu, K.L. Dorris, A. Shukla, Removal of nickel from aqueous solutions by sawdust, J. Hazard. Mater., 121 (2005) 243–246.
[52] B.A. Siddiqui, P.P. Sharma, M. Sultan, Adsorption studies on phosphate treated saw-dust: separation of Cr(VI) from Zn^{2+}, Ni^{2+} and Cu^{2+} and their removal and recovery from electroplating waste, Ind. J. Environ. Prot., 19 (1999) 846–852.
[53] I. Alomá, M.A. Martín-Lara, I.L. Rodríguez, G. Blázquez, M. Calero, Removal of nickel(II) ions from aqueous solutions by biosorption on sugarcane bagasse, J. Taiwan Inst. Chem. Eng., 43 (2012) 275–281.
[54] M. Torab-Mostaedi, H. Ghassabzadeh, M. Ghannadi-Maragheh, S.J. Ahmadi, H. Taheri, Removal of cadmium and nickel from aqueous solution using expanded perlite, Braz. *J.* Chem. Eng., 27 (2010) 299–308.
[55] M.E. Argun, S. Dursun, C. Ozdemir, M. Karatas, Heavy metal adsorption by modified oak sawdust: thermodynamics and kinetics, J. Hazard. Mater., 141 (2007) 77–85.
[56] S.R. Shukla, S.P. Roshan, Adsorption of Cu(II), Ni(II) and Zn(II) on dye loaded groundnut shells and sawdust, Sep. Purif. Technol., 43 (2005) 1–8.
[57] A. Kurniawan, A.N. Kosasih, J. Febrianto, Y.H. Ju, J. Sunarso, N. Indraswati, S. Ismadji, Evaluation of cassava peel waste as lowcost biosorbent for Ni-sorption: equilibrium, kinetics, thermodynamics and mechanism, Chem. Eng. J., 172 (2011) 158–166.
[58] H. Yu, J. Pang, T. Ai, L. Liu, Biosorption of Cu^{2+}, Co^{2+} and Ni^{2+} from aqueous solution by modified corn silk: equilibrium, kinetics, and thermodynamic studies, J. Taiwan Inst. Chem. Eng., 62 (2016) 21–30.
[59] P. Galiatsatou, M. Metaxas, V. Kasselouri-Rigopoulou, Adsorption of zinc by activated carbons prepared from solvent extracted olive pulp, J. Hazard. Mater., 91 (2002) 187–203.
[60] H.D. Doan, A. Lohi, V.B.H. Dang, T. Dang-Vu, Removal of Zn^{+2} and Ni^{+2} by adsorption in a fixed bed of wheat straw, Proc. Saf. Environ. Prot., 86 (2008) 259–267.
[61] X. Zhang, X. Wang, Adsorption and desorption of nickel(II) ions from aqueous solution by a lignocellulose/montmorillonite nanocomposite, PloS One, 10 (2015) e0117077.